

STRUCTURE OF LIGHT NEUTRON-RICH NUCLEI STUDIED WITH TRANSFER REACTIONS*

A.H. WUOSMAA

Department of Physics, University of Connecticut
Storrs, CT 06269-3046, USA

(Received January 16, 2015)

Transfer reactions have been used for many years to understand the shell structure of nuclei. Recent studies with rare-isotope beams extend this work and make it possible to probe the evolution of shell structure far beyond the valley of stability, requiring measurements in inverse kinematics. We present a novel technical approach to measurements in inverse kinematics, and apply this method to different transfer reactions, each of which probes different properties of light, neutron-rich nuclei.

DOI:10.5506/APhysPolB.46.627

PACS numbers: 21.10.-k, 25.40.Hi, 25.60.Je

1. Introduction

One of the main current thrusts of low-energy nuclear-structure research is to understand the evolution of shell structure away from the valley of stability. While many interesting features have been observed in heavier nuclei, the structures of neutron-rich light nuclei also reflect phenomena different from those near stability. The small binding energies and changes in the ordering of single-particle levels give rise to phenomena such as neutron halos, and can inform *ab initio* and shell-model calculations. Measurements on light nuclei accessible now can establish a basis for developing both experimental and theoretical methods that can be extended to more exotic systems. They can probe shell structure through the characterization of quantum numbers, spectroscopic factors and wave functions, and the effective single-particle energies.

* Presented at the Zakopane Conference on Nuclear Physics “Extremes of the Nuclear Landscape”, Zakopane, Poland, August 31–September 7, 2014.

Transfer reactions are among the methods most widely used to probe this behavior. With the advent of rare-isotope beams, these studies are now reaching well beyond stability (see, for example: [1–5]). Since the experiments must be carried out in inverse kinematics, these experiments face additional difficulties not encountered in measurements in normal kinematics. This paper will describe a novel experimental approach that addresses some of the problems associated with inverse kinematics, and present some examples of measurements that provide information about different aspects of the shell structure of light nuclei.

2. Inverse kinematics

In inverse kinematics, for a (d, p) reaction the interesting center-of-mass angles are transformed to backward angles in the laboratory, where the protons have small energies which can change rapidly with angle. The laboratory energy differences between protons from different excited states are also significantly smaller than those in the center-of-mass frame, resulting in a deterioration of the achievable center-of-mass energy resolution. For $(d, {}^3\text{He})$ and other similar reactions, the ejectiles are confined to forward laboratory angles, also with large shifts in energy with angle and multi-valued kinematic solutions. These kinematic shifts require detector arrays with fine segmentation to resolve narrowly spaced levels in the residual nuclei of interest.

2.1. The solenoid approach

Some of these problems can be alleviated by embedding the measurement in a strong, uniform magnetic field produced by a solenoid whose axis is aligned with the beam direction. The target is positioned roughly at the center of the solenoid. Light-charged particles emitted following transfer reactions follow helical cyclotron trajectories and, typically after one cyclotron period, return to the beam axis where they can be detected with a compact, linear array of position-sensitive silicon detectors (PSDs). These detectors measure the energy, distance from the target, and flight time of each particle. The flight time is approximately equal to the cyclotron period, which, in turn, is proportional to the mass-to-charge ratio, this information can be used for light-particle identification.

In this geometry, the kinematic correlations between particle energy and position are directly related to the center-of-mass energy and scattering angle. For a given state in the residual nucleus, the center-of-mass scattering angle is obtained from $\cos \theta_{\text{cm}} \propto z$, where z is the distance between target and detector (the “return distance”). The energy in the center-of-mass frame is also simply related to the laboratory energy and z by $E_{\text{lab}} = E_{\text{cm}} - A + Bz$, where A and B are constants determined by the bombarding energy, the

masses of the nuclei, and the magnetic-field strength. The kinematic shift is then the coefficient B which is typically between 15–40 keV/mm for a field of around 3 T. With the position resolution of the order of $\Delta z \approx 1$ mm, the excitation-energy resolution is not limited by kinematic shift. Also, the c.m. energy resolution is independent of position. This linear response simplifies the data analysis and improves the sensitivity for the weak transitions. These properties are the same for particles emitted in both forward and backward directions in the laboratory frame. More details about this approach can be found in [6].

2.2. HELIOS

This concept has been implemented at the ATLAS accelerator facility at Argonne National Laboratory with the HELical Orbit Spectrometer (HELIOS) [7]. HELIOS is built around a re-purposed superconducting magnetic resonance imaging solenoid with a maximum magnetic field of 2.85 T, bore diameter of approximately 1 m and bore length of 2.35 m. A 24-element PSD array surrounds the beam axis. Recoiling beam-like fragments are de-

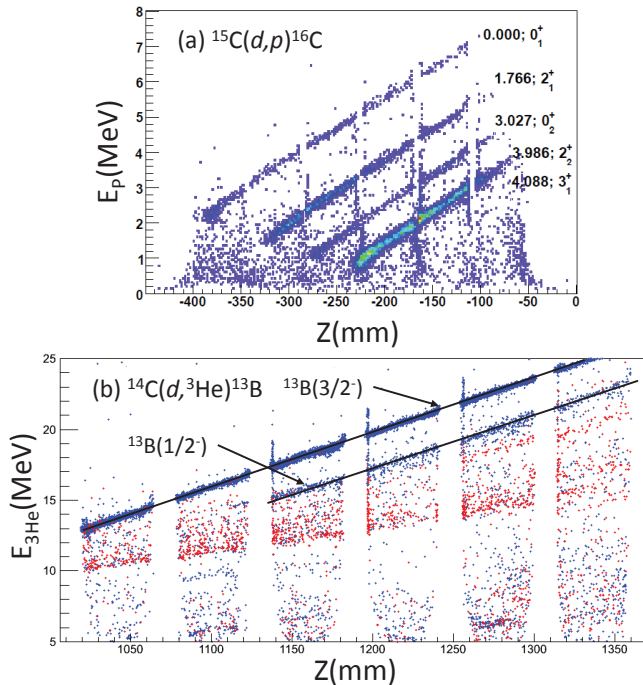


Fig. 1. Energy *versus* position correlations for (a) protons from the ${}^{15}\text{C}(d,p){}^{16}\text{C}$ reaction [10] and (b) ${}^3\text{He}$ from the ${}^{14}\text{C}(d,{}^3\text{He}){}^{13}\text{B}$ reaction. In (b), the dark grey (blue)/light grey (red) points represent coincidences with identified (${}^{13}\text{B}/{}^{12}\text{B}$) ions.

tected downstream of the target in arrays of silicon-detector telescopes, or using a high-rate gas ionization counter. The position-sensitive detector array can be placed to detect particles in either the backward or forward direction.

Examples of data that show the linear kinematic response of HELIOS appear in Fig. 1. Figure 1 (a) shows the proton energy as a function of position from a measurement of the $^{15}\text{C}(d,p)^{16}\text{C}$ reaction in inverse kinematics at a bombarding energy of 8.2 MeV/nucleon. The diagonal lines correspond to different excited states in the residual ^{16}C nucleus (see Ref. [10] for details). The recoiling ions were detected and identified in a set of silicon $\Delta E-E$ telescopes at forward angles. Similar data for the $^{14}\text{C}(d,^3\text{He})^{13}\text{B}$ reaction in inverse kinematics are shown in Fig. 1 (b). Here, the data for transitions to neutron-bound (dark grey, blue points) and neutron-unbound (light grey, red points) states are distinguished by the identification of the recoiling ^{13}B and ^{12}B ions with the $\Delta E-E$ telescopes in coincidence with the ^3He particles detected in the PSD array.

3. Physics examples with light, neutron-rich beams

3.1. *sd*-neutron states in ^{14}B

The neutron-rich isotope of boron ^{14}B is the lightest particle-bound $N = 9$ isotone. In ^{14}B , the $1s_{1/2}$ and $0d_{5/2}$ neutron strengths are fragmented due to coupling to the spin of the $0p_{1/2}$ proton, which produces a $(2,1)^-$ doublet for $1s_{1/2}$ and a $(1,2,3,4)^-$ multiplet for the $0d_{5/2}$ state. The residual interaction can also mix the s and d configurations in the 1^- and 2^- states. The s and d strengths in these levels can be determined by studying the $^{13}\text{B}(d,p)^{14}\text{B}$ reaction.

This measurement was conducted using a ^{13}B beam made with the $^9\text{Be}(^{14}\text{C},^{13}\text{B})^{10}\text{B}$ reaction at the in-flight radioactive-beam facility [8, 9] at the ATLAS accelerator laboratory at Argonne National Laboratory. The energy and intensity of the ^{13}B beam were 15.7 MeV/nucleon, and $\approx 30 \times 10^4$ particles per second, respectively. The beam bombarded a $200 \mu\text{g}/\text{cm}^2$ $(\text{CD}_2)_n$ foil. Protons were detected with the HELIOS PSD array, and recoiling $^{13,14}\text{B}$ nuclei were identified using the $\Delta E-E$ telescopes. Figure 2 shows the excitation-energy spectrum obtained from the measurement; the filled, and open histograms correspond to events where the proton was detected in coincidence with ^{14}B , and ^{13}B , respectively. The low-lying 2_1^- , 1_1^- , 3_1^- and 4_1^- states are observed. A broad 2^- excited state reported in the literature [11] at 1.86 MeV is likely obscured by the stronger 3^- and 4^- transitions. The angular distributions for the four low-lying narrow states appear in Fig. 3 (a), with curves that represent the results of distorted-wave Born approximation (DWBA) calculations. The optical-model parameters

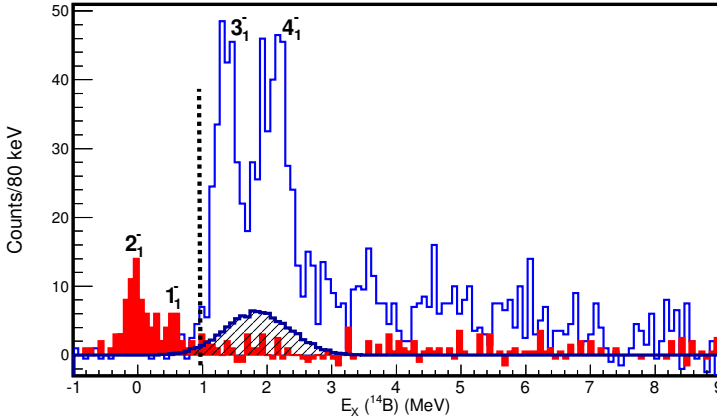


Fig. 2. Excitation-energy spectrum for the $^{13}\text{B}(d,p)^{14}\text{B}$ reaction. The filled histograms (red/open blue) correspond to particle bound/unbound states in ^{14}B , and the cross-hatched peak indicates where the broad excited 2_2^- state would appear in the spectrum. For details, see Ref. [12].

and a detailed discussion of the measurement and this analysis are given in Ref. [12]. The 3^- and 4^- transitions must be pure $\ell = 2$, however the 2^- and 1^- states can be populated by a mixture of $\ell = 0$ and 2 (dashed, and dot-dashed curves, respectively); the amount of mixing is determined by fitting the angular distributions to combinations of the DWBA curves for each ℓ value, with the resulting fit given by the solid curves in Fig. 3 (a) and (b). The ratios of the measured cross section to the resulting DWBA calculations

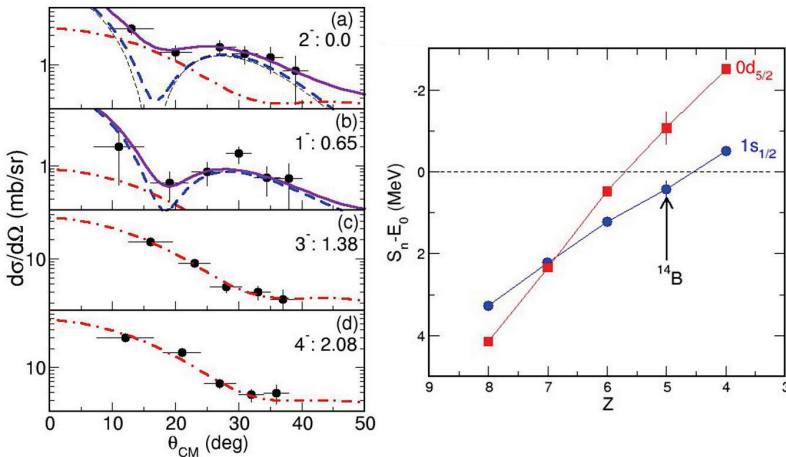


Fig. 3. Left: Proton angular distributions for the $^{13}\text{B}(d,p)^{14}\text{B}$ reaction. The curves represent DWBA calculations described in the text. Right: Z dependence of the $1s_{1/2}$ and $0d_{5/2}$ effective single-particle energies. For details, see Ref. [12].

provide an estimate of the relative spectroscopic strengths for the different transitions. These relative strengths are in good agreement with the predictions of shell-model calculations [12]. Using the experimental spectroscopic factors, and assuming the unobserved 2_2^- state is at 1.86 MeV (as suggested by the literature) and the 1_2^- is at 4.5 MeV as taken from the results of a shell-model calculation with the WBT interaction [13], the effective $1s_{1/2}$ and $0d_{5/2}$ single-particle energies can be obtained. The values are plotted in Fig. 3, with values for other $N = 9$ isotones. The present data fit well within the established trends. The deduced $1s_{1/2}$ - $0d_{5/2}$ splitting disagrees, however, with the values used in the different shell-model interactions, and could be used to provide guidance for improved shell-model interactions in the future.

3.2. Proton correlations in ^{14}C and the $^{14}\text{C}(d,^3\text{He})^{13}\text{B}$ reaction

A systematic dependence of the spectroscopic factors for nucleon removal on separation energy deduced from knockout reactions has been reported in Ref. [14], and was attributed to correlations in the ground states of light nuclei. An approach complementary to knock-out reactions to study such correlations is with nucleon-removal reactions such as $(d,^3\text{He})$ or (d,t) . In carbon isotopes, a previous study of the $^{12,13,14}\text{C}(d,^3\text{He})^{11,12,13}\text{B}$ reactions showed a smooth decrease in the number of non- $0p_{3/2}$ protons in the ground states of these C isotopes with increasing A [15]. The ^{14}C measurement was complicated by a large ^{12}C target impurity and weak transitions were obscured by contaminants. We have revisited this reaction in inverse kinematics, using HELIOS. Here, with a pure ^{14}C beam the measurement is sensitive to other weak transitions that may have evaded the earlier study.

Figure 4(a) shows the excitation-energy spectrum for the $^{14}\text{C}(d,^3\text{He})^{13}\text{B}$ reaction, measured with a 17.1 MeV/nucleon ^{14}C beam. The spectrum is dominated by the ground state, however weaker transitions are also observed. A presumed $1/2^-$ state reported by Mairle and Wagner at 3.71 MeV is present [15], and other excitations are seen near $E_X = 5.0$ and 6.2 MeV. A positive-parity state is suggested from the (t,p) reaction at 5.02 MeV [16], although another state nearby at 5.16 MeV has unknown J^π . Both are reported to decay by neutron emission while we observe coincidences with both ^{13}B and ^{12}B signifying both gamma-ray and neutron decays. Near 6 MeV, neutron-unbound levels near 6.17 and 6.43 are reported in the literature but with unknown J^π .

It is tempting to speculate about the nature of these weak transitions, which likely reflect particle-hole excitations out of the $\pi(0p_{3/2})^4\nu(0p)^6$ core. As concluded by Mairle and Wagner, the $1/2^-$ state in ^{13}B likely reflects a $\pi(0p_{1/2})^2$ component in ^{14}C . Another $3/2^-$ state could be produced by pro-

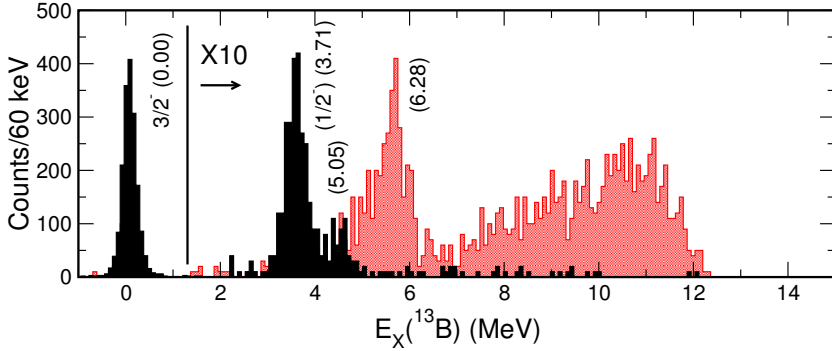


Fig. 4. Excitation-energy spectrum for the $^{14}\text{C}(d,^3\text{He})^{13}\text{B}$ reactions. The black and grey histograms correspond to particle bound, and unbound excitations, respectively.

ton removal from a $\pi(0p_{3/2})^4\nu(sd)^2$ ^{14}C component; the presence of neutron two-particle-two-hole (2p2h) admixtures in the ^{14}C ground-state wave function has been suggested by studies of the $^{14}\text{C}(d,t)^{13}\text{C}$ reaction [17] and the $^7\text{Li}(^7\text{Li},p)^{13}\text{B}$ reaction [18]. Similarly, positive-parity final states in ^{13}B must come from proton 2p2h admixtures in ^{14}C . Angular distributions for these transitions are still being analyzed, and will provide additional information about the nature of these excitations.

3.3. Aligned pn pair states in $^{12,13}\text{B}$ from the (d,α) reaction

Two-nucleon transfer reactions can be used to study pairing behavior in nuclei, and under certain circumstances have a high degree of selectivity for particular two-nucleon configurations. Two examples are the “deuteron-transfer” reactions (d,α) and (α,d) . The quantum numbers of the transferred pn pair are the same as those of the deuteron, namely $S = 1$ and $T = 0$, and these reactions have special affinity for populating so-called “aligned” states where the proton and neutron occupy orbitals with the same total angular momentum, and with their spins aligned forming the maximum possible value of $J = 2j$ [19]. The excitation probability for aligned configurations can be enhanced by the momentum mismatch, which favors a large transfer of angular momentum. This property was first exploited in the early 1960s to study high-spin excitations by the Berkeley group [20, 21]. Such states are difficult to populate with single-nucleon transfer reactions. Few, if any, examples of these pair transfer reactions with rare-isotope beams exist. In exotic nuclei, deuteron-removal reactions are of particular interest due to the different filling of proton and neutron orbitals. For light nuclei with large N/Z , the proton may be at the Fermi surface but the corresponding neutron can be tightly bound, putting the aligned state at high excitation energy.

We have used the deuteron-removal reactions $^{14,15}\text{C}(d, \alpha)^{12,13}\text{B}$, to study aligned pn hole configurations in $^{12,13}\text{B}$. The measurement was conducted using HELIOS in the same experimental configuration as for the $(d, ^3\text{He})$ reaction described above. For the ^{14}C beam, relatively weak transitions are expected to the ground and first-excited states in ^{12}B as the proton and neutron are removed from orbitals with different j , while the 3^+ state formed from the $(0p_{3/2})^2$ configuration should be strongly populated. Preliminary results for this reaction appear in Fig. 5 (a) and, as expected, the known 3^+ state at $E_X = 5.61$ MeV is strongly enhanced. The 1^+ and 2^+ ground and first-excited states are only weakly populated.

Figure 5 (b) shows the corresponding results with the unstable ^{15}C beam. A simple interpretation of the $^{15}\text{C}(d, \alpha)^{13}\text{B}$ reaction is that the removed pn pairs are the same as those transferred from ^{14}C , with the additional $1s_{1/2}$ neutron in ^{15}C acting as a spectator. In this case, the ground state is only barely on the HELIOS acceptance, and we see evidence for the population of members of a previously reported multiplet of states near 3.5 MeV. Additional strength is observed for levels between 4 and 10 MeV, although relatively little spin-parity information is available for states above 5 MeV excitation energy in ^{13}B . The most prominent feature in the spectrum is a possible doublet of states near $E_X = 12$ MeV ($Q \approx -8$ MeV); it is most likely that this structure corresponds to the aligned 3^+ configuration in ^{12}B coupled to the $1s_{1/2}$ valence neutron, forming a doublet with $J^\pi = (5/2, 7/2)^+$. More guidance about the possible structure of these states can be found

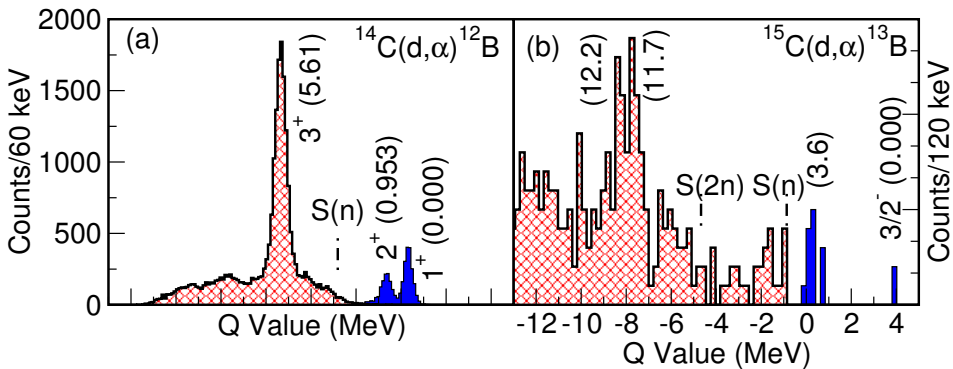


Fig. 5. Q -value spectra for the $^{14}\text{C}(d, \alpha)^{12}\text{B}$ (a) and $^{15}\text{C}(d, \alpha)^{13}\text{B}$ (b) reactions.

by comparing the angular distributions for the transitions to states in ^{12}B with that of the 12 MeV doublet structure. Figure 6 shows angular distributions for the $(1, 2, 3)^+$ states in ^{12}B , as well as that for the structure in ^{13}B (Fig. 6 (c)). While the angular distributions for the $^{12}\text{B}(1, 2)^+$ transitions

are strongly peaked, the $^{12}\text{B}(3^+)$ angular distribution is relatively featureless. The angular distribution for the ^{13}B structure at $E_X \approx 12$ MeV is very similar to that for the $^{12}\text{B}(3^+)$ case, as would be expected if the mechanism were the same for the two reactions. Such a comparison supports the interpretation of this feature as an aligned pn -hole pair.

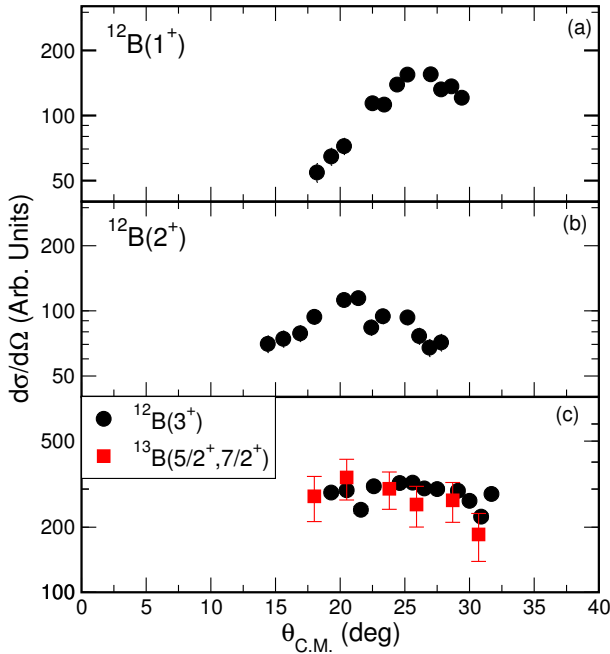


Fig. 6. Angular distributions for the $(1,2,3)^+$ transitions in the $^{14}\text{C}(d, \alpha)^{12}\text{B}$ reaction. Data for the ^{13}B doublet are the square symbols in (c).

4. Summary and conclusions

These results illustrate how single- and multi-nucleon transfer reactions can be carried out with radioactive beams to provide guidance for shell-model calculations in light nuclei. Results from neutron-adding reactions reflect the evolution of effective single-particle energies with increasing N/Z ratio, and one- and two-nucleon removal reactions can be used to probe correlations, and states with special character that have not yet been closely studied in exotic nuclei. With the coming availability of new facilities that can provide Coulomb-barrier energy beams of very neutron-rich nuclei, there are many new opportunities for extending these studies to even more exotic systems.

The author wishes to thank J.P. Schiffer for many helpful discussions. This work was supported by the U.S. Department of Energy, Office of Nuclear Physics, under Contracts DE-FG02-04ER41320 and DE-AC02-06CH11357, and the U.S. National Science Foundation under Grant No. PHY-1068217.

REFERENCES

- [1] H. Jeppeson *et al.*, *Phys. Lett.* **B645**, 17 (2006).
- [2] R.L. Kozub *et al.*, *Phys. Rev.* **C73**, 044307 (2006).
- [3] W.N. Catford *et al.*, *Phys. Rev. Lett.* **104**, 192501 (2010).
- [4] K.L. Jones *et al.*, *Nature* **465**, 454 (2010).
- [5] B. Fernández-Dominguez *et al.*, *Phys. Rev.* **C84**, 011301(R) (2011).
- [6] A.H. Wuosmaa *et al.*, *Nucl. Instrum. Methods Phys. Res.* **A580**, 1290 (2007).
- [7] J.C. Lighthall *et al.*, *Nucl. Instrum. Methods Phys. Res.* **A622**, 97 (2010).
- [8] B. Harss *et al.*, *Rev. Sci. Instrum.* **71**, 380 (2000).
- [9] K.E. Rehm *et al.*, *Nucl. Instrum. Methods Phys. Res.* **A647**, 3 (2011).
- [10] A.H. Wuosmaa *et al.*, *Phys. Rev. Lett.* **105**, 132501 (2010).
- [11] F. Azjenberg-Selove, *Nucl. Phys.* **A523**, 1 (1991).
- [12] S. Bedoor *et al.*, *Phys. Rev.* **C88**, 011304(R) (2013).
- [13] E.K. Warburton, B.A. Brown, *Phys. Rev.* **C46**, 923 (1992).
- [14] A. Gade *et al.*, *Phys. Rev.* **C77**, 044306 (2008).
- [15] G. Mairle, G.J. Wagner, *Nucl. Phys.* **A253**, 253 (1975).
- [16] R. Middleton, D.J. Pullen, *Nucl. Phys.* **51**, 50 (1964).
- [17] H. Weller *et al.*, *Phys. Rev.* **C13**, 38 (1976).
- [18] H. Iwasaki *et al.*, *Phys. Rev. Lett.* **102**, 202502 (2009).
- [19] N.K. Glendenning, *Annu. Rev. Nucl. Part. Sci.* **13**, 191 (1963).
- [20] R.H. Pehl, E. Rivet, J. Cerny, B.G. Harvey, *Phys. Rev.* **137**, B114 (1965).
- [21] E. Rivet, R.H. Pehl, J. Cerny, B.G. Harvey, *Phys. Rev.* **141**, 1021 (1966).